ISBN: 978-3-95450-229-5 ISSN: 2673-5520 doi:10.18429/JACoW-MEDSI2020-TUOB01

EXACTLY-CONSTRAINED KB MIRRORS FOR SIRIUS/LNLS BEAMLINES: DESIGN AND COMMISSIONING OF THE TARUMÃ STATION NANOFOCUSING OPTICS AT CARNAÚBA BEAMLINE

G. B. Z. L. Moreno†, R. R. Geraldes, C. S. N. C. Bueno, F. R. Lena, S. A. L. Luiz, Y. R. Tonin, E. O. Pereira, W. H. Wilendorf, H. C. N. Tolentino, Brazilian Synchrotron Light Laboratory (LNLS), Brazilian Centre for Research in Energy and Materials (CNPEM), Campinas, SP, Brazil

Abstract

Next-generation nanoprobes, empowered by diffraction-limited storage rings, as Sirius at the Brazilian Synchrotron Light Source (LNLS), present high-performance requirements aiming at high spatial resolution and throughput. For the focusing optics, this means assuring a small and non-astigmatic probe, high flux density, and remarkably high position stability, while simultaneously preserving beam wavefront. At stations further dedicated to spectromicroscopy and *in-situ* experiments, these requirements add up to having achromatic design and suitable working distance, respectively. In this way, Kirkpatrick-Baez (KB) mirrors have been chosen as an appropriate solution for many of Sirius focusing optics. Yet, the consequent requirements on mirror angular stability in less than 10 nrad RMS, surface quality in single-digit nanometers, and alignment tolerances in the range of hundreds of nanoradians, are particularly challenging regarding clamping, vibration, and thermal expansion budgets, even exceeding optical metrology limits. This work discusses the specifications, design concept, and assembly aspects of the new KB systems for Sirius, taking the TARUMÃ station from CARNAÚBA beamline as a case study with its early commissioning results.

INTRODUCTION

The design of efficient X-ray nanofocusing systems, with high mechanical stability and optimized compatibility with progressively ambitious experimental setups, is an investment of significant potential in spatial and temporal resolution, especially when fully utilizing the brightness and coherence of 4th-generation light sources [1]. Achromaticity, large working distances, and higher acceptance guided the choice for Kirkpatrick-Baez (KB) mirrors as the nanofocusing optics for many stations at Sirius [2].

TARUMÃ [3] is a sub-microprobe dedicated to multi-technique microscopy and spectroscopy experiments in the energy range of 2.05 to 15 keV in *in-situ* and *in-operando* conditions at CARNAÚBA (Coherent X-Ray Nanoprobe Beamline) [4, 5]. Starting commissioning in December 2020, it is the first nanoprobe at Sirius, where a KB focuses x-rays to 120 nm spot sizes (>8 keV) with 450 mm working distance and up to 1e11 ph/s/100mA on the sample.

Although very promising for scientific opportunities, this optical design brings remarkably strict requirements in manufacturing, installation, and positioning. This is clear from the short summary in Table 1, which includes the forthcoming station at MOGNO and the SAPOTI station at CARNAÚBA, with even tighter specifications. Hence, a high-stability KB system, built on precision engineering concepts and following a predictive design approach, has been developed in-house. The first system, built for TARUMÃ, is also as a proof of concept for the next KB sets.

Table 1: Short Specifications for the First Sirius KB Sets

KB set	TARUMÃ	MOGNO	SAPOTI
Focus size	120 nm	100 nm	35 nm
Dep. of Focus	80 µm	20 µm	5 µm
Max. Mir. Len.	210 mm	450 mm	390 mm
Work. Distance	450 mm	175 mm	55 mm
Grazing Angle	3.9 mrad	4.0 mrad	3.9 mrad
Pitch stability	<10 nrad	< 10 nrad	< 4 nrad
Surface Error	< 1 nm	< 1 nm	< 1 nm

CONCEPT AND DESIGN

As compared with other X-ray focalizing elements, such as zone plates and refractive lenses, KB systems can be used in achromatic optical designs, reach larger working distances, and eventually allow for higher acceptance [6]. On the other hand, when also bounded to high numerical apertures and small grazing angles, mirrors are longer and heavier components, which are more difficult to handle and position, often resulting in limited dynamics. Moreover, apart from small focalizing elements, relative metrology over the extense mirror substrates and/or between the optics and the sample gets complicated. At TARUMÃ, for instance, where the KB set is in Ultra-High-Vacuum and the sample is in open-atmosphere, metrology with sufficient accuracy would be hardly even possible (see [7]).

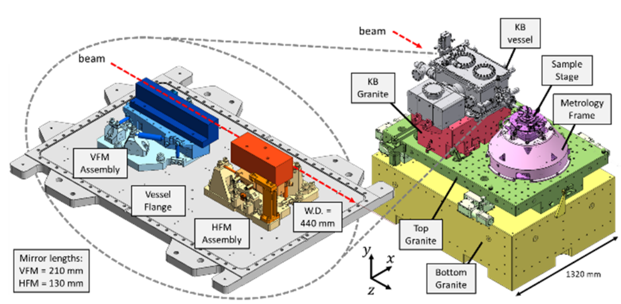

Figure 1: Reduced drawings of experimental bench and KB set with VFM and HFM assemblies in the vacuum vessel.

Building up from previous KB system and mirror base designs [8-12], and recent developments in primary optics for Sirius mirror systems [13], a deterministic design for passive high-stability performance was implemented for KB systems. The concept relies in maximizing the suspension frequency of both mirrors with respect to a single

ISBN: 978-3-95450-229-5 ISSN: 2673-5520 doi:10.18429/JACoW-MEDSI2020-TUOB01

reference frame, which can be directly shared with the sample stage or used as a metrology reference for it. With high suspension modes, the sensitivity to common mechanical disturbances is reduced, which, together with proper management of vibrational disturbances, allows for reducing displacement errors to a few nanometers. As illustrated in Fig. 1, for TARUMÃ this reference frame is the top granite of the experimental bench itself.

Sensitivity Analysis and Actuation Ranges

The design premise was to keep the internal mechanism as simple and stiff as possible. Thus, an error sensitivity analysis of each elliptical mirror permitted taking profit from the orthogonal nature of the KB set, and the fact that each mirror is shaped only in one direction. Error tolerances could be shared among both mirrors, and a better use of mounting tolerances, motion range, and actuator placement could be applied, avoiding unnecessary loss of support stiffness. Table 2 shows the alignment specs for each mirror regarding position tolerance for the focus: the maximum misalignment allowed in the transversal (Tx,Ty) and longitudinal (Z) axes was 10% of the focus size (σ) and depth (DF), respectively. Additionally, the last lines refer to the alignment and stability of the full set around each mirror reference point, considering that the sample and mirror move together on top of the same bench:

Table 2: Tarumã KB Alignment Specifications

Alignment specification	**VFM**	**HFM**
Pitch error tol. (mirror to sample)	4 µrad	15 µrad
Roll error tol. (mirror to mirror)	50 µrad	50 µrad
Yaw error tol. (mirror to mirror)	>1 mrad	>1 mrad
Pitch @ T=10% σ (stability)	7 nrad	10 nrad
Pitch @ Z=10% DF (astigmat.)	0.4 µrad	0.7 µrad
Pitch @ σ=110% σ_0 (coma)	4 µrad	15 µrad
Focus Z @ max pitch allowed	~1 mm	~2 mm
KB set Pitch stability (to source)	14 nrad	20 nrad
KB set Tx/Ty stability (to source)	2 µm	2 µm
KB set Roll angle (to source)	>2 mrad	---

This way, only two actuation axes are implemented inside vacuum: the VFM pitch, for compensating possible mounting errors making the focus astigmatic, and the HFM roll, for correcting perpendicularity between the mirrors. All other actuation axes are covered by the 6-DoF granite bench that moves the entire KB set and the sample together.

Exactly-Constrained Design

To optimize vibration modes by reducing mass in the mirror frame, reinforced struts were used to exactly constrain each mirror frame instead of the folded leaf-springs used in [13]. This granted a significant size reduction since the mounting volumes for struts are far more compact. The center of gravity of the mirror-frame assembly was optimized to be as close as possible to the stiffness center of the struts, improving suspension frequencies to >450 Hz and the most sensitive mode to >1 kHz. Although this choice led to larger parasitic motion, from strut shortening effects, and reduced range/stiffness ratio, both aspects were authorized by the sensitivity analysis mentioned in the previous section. For the in-vacuum actuation, an N-470 Piezo-Mike and a PiRest P-888.31 by PI were chosen for the HFM-roll and VFM-pitch actuation, respectively. For feedback, Lion Precision capacitive probes were used. The detailed design of the mirror mechanics is shown in Fig. 2.

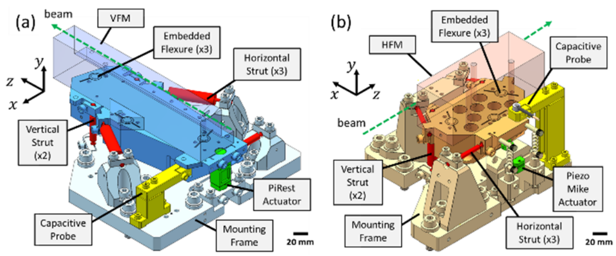

Figure 2: KB mechanisms for VFM (a) and HFM (b), highlighting embedded flexures in the frames reinforced flexural struts, piezo actuators and capacitive sensors.

As with the primary optics, deformations from thermal expansion mismatch are mitigated by having the mirrors fixed to three embedded flexures in the mirror frames, creating a thermal center. As an additional measure, the KB frames were made from a custom Invar alloy with a thermal expansion coefficient (CTE) closer to that of silicon at room temperature. The special Invar is a modified ASTM B743 Invar 37 re-forged with a Ni concentration of 37.5%, resulting in a tested CTE of 3.12 (µm/m)/K at 35°C.

Next, ensuring high-stiffness links between the KB mirrors and their fixtures was mandatory to preserve the high suspension coupling to the granite bench and minimizing the errors in the passive stability or metrology. However, the common approach of bolting or clamping mirrors to their mounts would be impracticable for KB mirrors, as the required preload forces would introduce unacceptable deformations at the optical surfaces, affecting focus [14]. The solution consisted of epoxy-gluing the mirrors to the embedded flexures in the frames, such that, not only clamping forces are prevented, but also the hinges in [13] are expendable, with the interface stiffness becoming limited only by the adhesive elastic modulus, the bond layer thickness and interface area. A mixture of MasterBond 42HT-2LO epoxy adhesive with embedded 53 µm glass microspheres (1% w.t.) is deposited over the three 8 mm diameter pads with a custom dispenser. The resulting bond layer has a reproducible 60µm interface thickness that is dominated by the spheres when preloaded by the mirrors weight.

To quantitatively evaluate the residual bond layer shear stresses from epoxy cure-induced contraction that could deform the mirror surface, deformations in 1mm thick glass slides glued to a metal substrate were measured during the curing process and fed to a custom material model in Ansys Mechanical. This model allowed some optimization of the interface area diameter by finding a suitable compromise between stiffness and adhesion strength in the point of maximum shear stresses. Figure 3 shows the simulated comparison between the deformation profiles of a 120N bolted solution and the glued interfaces (both with

ISBN: 978-3-95450-229-5 ISSN: 2673-5520 doi:10.18429/JACoW-MEDSI2020-TUOB01

estimated stiffness > 1e9 N/m), with the maximum values of 0.47 nm for the HFM and 2.3 nm for the VFM in the latter case, and the effects on the HFM focus profile.

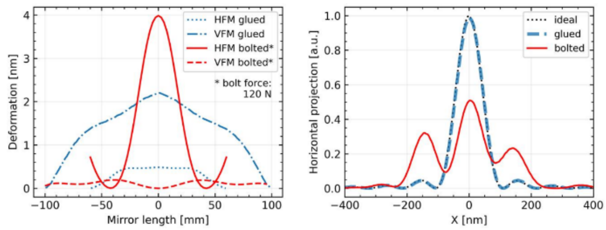

Figure 3: VFM and HFM surface deformations (left) and given HFM focus profiles (right) for different fixture types.

METROLOGY AND ASSEMBLY

Resulting from the design decisions stated previously, much engineering effort was transferred to the assembly phase, when the preliminary alignment of the KB set had to be done offline and with paramount precision. If the alignment between mirrors was to fall off the limits stated in Table 2, the specified in-vacuum motion ranges would become insufficient for an acceptable focus alignment in 2D. Therefore, in addition to confirming mirror figure, a proper fiducialization of such figure within space was mandatory for an adequate alignment of the KB set with regard to the sample at the experimental station.

A sequence of measurements with a Fizeau interferometer (FZI) setup was conducted to confirm figure error contributions from the gluing process. However, due to repeatability limits and height errors of the interferometric lens, the measurement error was limited to about 3 nm peak-to-valley, still above the expected surface deformations. Thus, ultimate validation remained for commissioning with the X-ray beam at the beamline.

Concerning alignment, the orientation of each mirror ellipse in their own substrate was estimated from fitting points at the side of the polished areas, measured with about 1 µm resolution in a Zeiss coordinate measurement machine (CMM). The fitting algorithm used Python's *lmfit* library to perform a least-squares fit of the center and rotation angle of a fixed ellipse that generated from the p, q and θ design parameters obtained from the manufacturer's documentation. This assessment provided enough information to manufacture parts compensating deviations in the mirror substrate, allowing a more assertive assembly of the mechanics. The vacuum chamber was specially designed to fit within the CMM working volume, so the assembly could be metrology-assisted. A simultaneous setup with 6 length gauges provided a 6-DoF position-feedback of each mirror, mounted and adjusted with complementary structures. The VFM height and angle was aligned to the vessel base flange, whereas the HFM height and angle was aligned to the VFM axis. Lastly, the longitudinal position of the HFM was aligned to the VFM fitted focus.

To conclude, still in the CMM, the KB fitted focus was fiducialized to targets outside the vacuum chamber, used later for the experimental station laser tracker alignment. The final mounting errors for the KB are listed in Table 3.

Table 3: KB Set Assembly Uncertainties with the CMM

Mirror Axis	Ellipse Fit	CMM Uncertainty	HFM to VFM Mount Error*
Tx	50 µm	1 µm	15 ± 50 µm
Ty	70 µm	1 µm	15 ± 70 µm
Tz	164 µm	1 µm	8 ± 164 µm
Rx	3 µrad	15 µrad	40 ± 15 µrad
Ry	1 µrad	15 µrad	105 ± 15 µrad
Rz	---	67 µrad	215 ± 67 µrad

COMMISSIONING

After the preliminary alignment campaign during installation, the alignment of the KB set with respect to the beam is done by jointly moving the experimental bench and searching for the focus with a reference sample, done at TARUMÃ via knife-edge fluorescence mapping or ptychographic reconstructions. The alignment strategy consists in firstly aligning the HFM and VFM to the source, correcting coma aberrations with the Ry and Rx DoFs in the KB granite and top granite, respectively. Next, the fine VFM coma, and astigmatism and trefoil aberrations between mirrors are corrected with the internal actuators. Figure 4 shows the preliminary results obtained with x-rays at TARUMÃ:

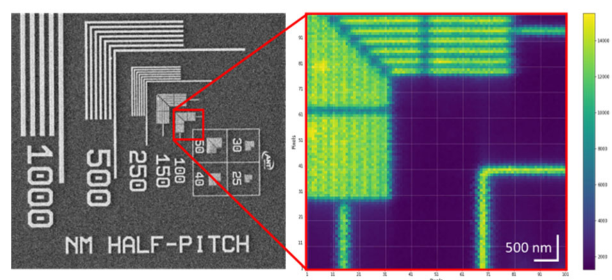

Figure 4: Applied Nanotools 100 nm calibration patterns (left) imaged by pink beam fluorescence mapping (right).

CONCLUSION

Although commissioning is still ongoing, the preliminary results of the first KB system following the innovative in-house design at TARUMÃ suggest that the ambitious design targets have been achieved. Although close to the limits of the instruments, the new dimensional metrology procedure proved successful. The optical metrology, however, needs even further improving, where a calibration of the lens and a more robust setup are underway, considering the validation of next KB systems. The sensitivity analysis paves the way to more optimized designs, considering not only better use of mounting and alignment tolerances, but also allowing high-dynamic realizations. The lessons learned at TARUMÃ already benefit the new designs with more challenging specs underway, including multiple coating stripes and even stricter stability tolerances.

ACKNOWLEDGEMENTS

The authors would like to gratefully acknowledge the funding by the Brazilian Ministry of Science, Technology

ISBN: 978-3-95450-229-5 ISSN: 2673-5520 doi:10.18429/JACoW-MEDSI2020-TUOB01

and Innovation, the contributions of the LNLS team and partners, and the participation of the MI-Partners in the SAPOTI project, with fruitful feedback to TARUMÃ.

REFERENCES

[1] M. Eriksson, J. Friso, V. der Veen, and C. Quitmann, "Diffraction-limited storage rings – a window to the science of tomorrow," *J. Synchrotron Rad.*, vol. 21, pp. 837–842, 2014. doi: 10.1107/S1600577514019286

[2] A. R. D. Rodrigues *et al.*, "Sirius Status Update," in *Proc. IPAC'19,* Melbourne, Australia, May 2019, pp. 1381-1384. doi:10.18429/JACoW-IPAC2019-TUPGW003

[3] H. Tolentino *et al.*, "TARUMÃ station for the CARNAUBA beamline at SIRIUS/LNLS," in *Proc. SPIE Optical Engineering and Applications*, vol. 11112, X-Ray Nanoimaging: Instruments and Methods IV, p. 1111206, 2019. doi:10.1117/12.2531110

[4] H. C. N. Tolentino *et al.*, "CARNAÚBA : the coherent x-ray nanoprobe beamline for the Brazilian synchrotron SIRIUS / LNLS," *IOP Conf. Ser.: J. Phys.*, vol. 849, no. 1, p. 012057, 2017. doi:10.1088/1742-6596/849/1/012057

[5] H. C. N. Tolentino *et al.*, "X-ray microscopy developments at Sirius-LNLS: first commissioning experiments at the Carnaúba beamline," in *Proc. SPIE Optical Engineering and Applications*, vol. 11839, X-Ray Nanoimaging: Instruments and Methods V, p. 1183904, 2021. https://doi.org/10.1117/12.2596496

[6] X. Shi, R. Reininger, R. Harder, and D. Haeffner, "X-ray optics simulation and beamline design for the APS upgrade," in *Proc. SPIE Optical Engineering and Applications*, vol. 10388, Advances in Computational Methods for X-Ray Optics IV, p. 103880C, 2017. doi:10.1117/12.2274571

[7] R. R. Geraldes *et al.*, "Design and commissioning of the TARUMÃ station at the CARNAÚBA beamline at SIRIUS/ LNLS" presented at the 11th Int. Conf. on Mechanical Engineering Design of Synchrotron Radiation Equipment and Instrumentation (MEDSI2020), Chicago, IL, USA, virtual conference, July 2021, paper WEPB13, this conference.

[8] R. Barrett *et al.*, "Reflective optics for hard x-ray nanofocusing applications at the ESRF," *Synchrotron Radiat. News*, vol. 29, no. 4, pp. 10-15, 2016. doi:10.1080/08940886.2016.1198668

[9] T. Goto *et al.*, "Hard X-ray nanofocusing using adaptive focusing optics based on piezoelectric deformable mirrors," *Rev. Sci. Instrum.*, vol. 86, no. 4, pp. 1-7, 2015. doi:10.1063/1.4916617

[10] R. Baker *et al.*, "New generation mirror systems for ESRF upgrade beamlines," *J. Phys. Conf. Ser.*, vol. 425, no. 5, p. 052015, 2013. doi:10.1088/1742-6596/425/5/052015

[11] C. Preissner *et al.*, "Earth, wind, and fire: the new fast scanning velociprobe," in *Proc. MEDSI'16,* Barcelona, Spain, Sep. 2016, pp. 112-115. doi:10.18429/JACoW-MEDSI2016-TUAA02

[12] R. R. Geraldes *et al.*, "Granite benches for SIRIUS x-ray optical systems," in *Proc. MEDSI'18*, Paris, France, Jun. 2018, pp. 361-364. doi:10.18429/JACoW-MEDSI2018-THPH12

[13] R. R. Geraldes *et al*., "The design of exactly-constrained x-ray mirror systems for SIRIUS," in *Proc. MEDSI'18*, Paris, France, Jun. 2018, pp. 173-178. doi:10.18429/JACoW-MEDSI2018-WEOAMA04

[14] L. M. Volpe *et al*., "Optimization method using thermal and mechanical simulations for SIRIUS high-stability mirrors," in *Proc. MEDSI'18*, Paris, France, Jun. 2018, pp. 273-276. doi:10.18429/JACoW-MEDSI2018-WEPH31